Biochimica et Biophysica Acta 1797 (2010) 1727–1735

Contents lists available at ScienceDirect

Biochimica et Biophysica Acta

journal homepage: www.elsevier.com/locate/bbabio

The dynamics of mitochondrial Ca^{2+} fluxes

Sergio de la Fuente, Pablo Montenegro, Rosalba I. Fonteriz, Alfredo Moreno, Carmen D. Lobatón, Mayte Montero, Javier Alvarez *

Instituto de Biología y Genética Molecular (IBGM), Departamento de Bioquímica y Biología Molecular y Fisiología, Facultad de Medicina, Universidad de Valladolid and Consejo Superior de Investigaciones Científicas (CSIC), Ramón y Cajal, 7, E-47005 Valladolid, Spain

ARTICLE INFO

Article history:
Received 19 February 2010
Received in revised form 10 June 2010
Accepted 17 June 2010
Available online 25 June 2010

Keywords:
Ca^{2+} fluxes
Ca^{2+} dynamics
Ca^{2+} buffering
Mitochondria
Aequorin

ABSTRACT

We have investigated the kinetics of mitochondrial Ca^{2+} influx and efflux and their dependence on cytosolic $[Ca^{2+}]$ and $[Na^+]$ using low-Ca^{2+}-affinity aequorin. The rate of Ca^{2+} release from mitochondria increased linearly with mitochondrial $[Ca^{2+}]$ ($[Ca^{2+}]_M$). Na^+-dependent Ca^{2+} release was predominant al low $[Ca^{2+}]_M$ but saturated at $[Ca^{2+}]_M$ around 400 μM, while Na^+-independent Ca^{2+} release was very slow at $[Ca^{2+}]_M$ below 200 μM, and then increased at higher $[Ca^{2+}]_M$, perhaps through the opening of a new pathway. Half-maximal activation of Na^+-dependent Ca^{2+} release occurred at 5–10 mM $[Na^+]$, within the physiological range of cytosolic $[Na^+]$. Ca^{2+} entry rates were comparable in size to Ca^{2+} exit rates at cytosolic $[Ca^{2+}]$ ($[Ca^{2+}]_c$) below 7 μM, but the rate of uptake was dramatically accelerated at higher $[Ca^{2+}]_c$. As a consequence, the presence of $[Na^+]$ considerably reduced the rate of $[Ca^{2+}]_M$ increase at $[Ca^{2+}]_c$ below 7 μM, but its effect was hardly appreciable at 10 μM $[Ca^{2+}]_c$. Exit rates were more dependent on the temperature than uptake rates, thus making the $[Ca^{2+}]_M$ transients to be much more prolonged at lower temperature. Our kinetic data suggest that mitochondria have little high affinity Ca^{2+} buffering, and comparison of our results with data on total mitochondrial Ca^{2+} fluxes indicate that the mitochondrial Ca^{2+} bound/Ca^{2+} free ratio is around 10- to 100-fold for most of the observed $[Ca^{2+}]_M$ range and suggest that massive phosphate precipitation can only occur when $[Ca^{2+}]_M$ reaches the millimolar range.

1. Introduction

Mitochondrial Ca^{2+} fluxes play a very important role in cell physiology. The large negative potential of the mitochondrial matrix provides an enormous driving force for Ca^{2+} entry through the inner mitochondrial membrane. However, $[Ca^{2+}]_M$ is low under resting conditions because of the very low Ca^{2+} permeability of the inner mitochondrial membrane and the operation of systems able to extrude Ca^{2+} from mitochondria in exchange by Na^+ or H^+. During cell activation, the increase in $[Ca^{2+}]_c$ triggers the opening of the mitochondrial Ca^{2+} uniporter, a Ca^{2+} channel of the inner mitochondrial membrane, and large amounts of Ca^{2+} flow through this channel into the mitochondrial matrix. Opening of the uniporter is thus triggered by cytosolic Ca^{2+}, but its activation requires relatively high $[Ca^{2+}]_c$, with Kd values for the activation in the range 20–50 μM [1–9].

During physiological cell activation, $[Ca^{2+}]_c$ never usually rises above 1–2 μM, except for some small regions close to the Ca^{2+} channels. Nevertheless, because the maximum Ca^{2+} flux through the uniporter is very big, even a small degree of opening of the uniporter is able to induce a significant Ca^{2+} entry into mitochondria. This situation of submaximal activation of the uniporter is the most frequent under physiological conditions, and balance between influx and efflux pathways should then be critical to determine the final $[Ca^{2+}]_M$. However, there is little direct information on the kinetics of mitochondrial Ca^{2+} fluxes obtained by looking directly at $[Ca^{2+}]_M$. We have investigated here in detail the behaviour of mitochondrial Ca^{2+} fluxes under different conditions of extramitochondrial $[Ca^{2+}]$, $[Na^+]$ and temperature to obtain a clearer picture of mitochondrial $[Ca^{2+}]$ homeostasis.

2. Methods

2.1. Cell culture and targeted aequorin expression

HeLa cells were grown in Dulbecco's modified Eagle's medium supplemented with 5% fetal calf serum, 100 i.u.ml^{-1} penicillin and 100 i.u.ml^{-1} streptomycin. The construct for mutated aequorin targeted to mitochondria (mitmutAEQ) has been described previously [4]. Transfections were carried out using Metafectene (Biontex, Munich, Germany).

2.2. $[Ca^{2+}]_M$ measurements with aequorin

HeLa cells were plated onto 13 mm round coverslips and transfected with the plasmid for mitochondrially targeted mutated

Abbreviations: $[Ca^{2+}]_c$, cytosolic $[Ca^{2+}]$; $[Ca^{2+}]_M$, mitochondrial $[Ca^{2+}]$; mitmutAEQ, mutated aequorin targeted to mitochondria

* Corresponding author. Tel.: +34 983 423085; fax: +34 983 423588.
E-mail address: jalvarez@ibgm.uva.es (J. Alvarez).

0005-2728/$ – see front matter © 2010 Elsevier B.V. All rights reserved.
doi:10.1016/j.bbabio.2010.06.008

aequorin. For aequorin reconstitution, HeLa cells were incubated for 1–2 h at room temperature in standard medium (145 mM NaCl, 5 mM KCl, 1 mM $MgCl_2$, 1 mM $CaCl_2$, 10 mM glucose, and 10 mM HEPES, pH 7.4) with 1 μM of coelenterazine n. After reconstitution, cells were placed in the perfusion chamber of a purpose-built luminometer. Then, standard medium containing 0.5 mM EGTA instead of Ca^{2+} was perfused for 1 min, followed by 1 min of intracellular medium (130 mM KCl, 10 mM NaCl, 1 mM $MgCl_2$, 1 mM potassium phosphate, 0.5 mM EGTA, 1 mM ATP, 20 μM ADP, 10 mM L-malate, 10 mM glutamate, 10 mM succinate, 20 mM Hepes, pH 7) containing 100 μM digitonin. Then, intracellular medium without digitonin was perfused for 5–10 min, followed by buffers of known [Ca^{2+}] prepared in intracellular medium using HEDTA/Ca^{2+}/Mg^{2+} mixtures. To obtain intracellular mediums with different [Na^+], the concentration of Na^+ in the medium was equimolarly replaced by K^+. Temperature was set either at 22 °C or at 37 °C.

Calibration of the luminescence data into [Ca^{2+}] was made using an algorithm as previously described [10,11]. Calibration of mutated aequorin reconstituted with coelenterazine n has been previously made at pH 7 under three different conditions: *in vitro* [12], inside the endoplasmic reticulum [10,12] and inside mitochondria [13]. The relationship between relative luminescence and [Ca^{2+}] was the same in all the cases, indicating that the response of aequorin to Ca^{2+} was not altered inside any of these organelles. However, given that the resting pH inside mitochondria in HeLa cells is known to be close to 8 [14,15], the values obtained with the pH 7 calibration require a 20% downwards correction, as we have recently described [13]. [Ca^{2+}] values in this paper have therefore been obtained using the original pH 7 calibration and applying then this small correction.

2.3. Measurement of total calcium uptake by HeLa cell mitochondria

Isolation of mitochondria from HeLa cell was carried out using the Mitochondria Isolation kit from Miltenyi Biotec (Bergisch Gladbach, Germany). Mitochondria were treated with 1 μM thapsigargin to block SERCA pumps and they were finally suspended in intracellular medium containing 5 μM EGTA and assayed for protein concentration using the Pierce BCA protein assay kit (Thermo Fischer Scientific, Waltham, MA, USA). The yield in terms of mitochondrial protein was approximately 1 mg/10^8 cells. To measure calcium uptake, 0.1 mg of mitochondrial protein were suspended in 1 ml of intracellular medium containing 5 μM EGTA and 0.3 μM Calcium Green-5 N (Molecular Probes) and incubated at 37 °C under magnetic stirring in the cuvette holder of an Aminco-Bowman series 2 fluorescence spectrophotometer. Fluorescence excited at 506 nm and emitted at 532 nm was monitored and then 20 nmol of calcium was added to start mitochondrial Ca^{2+} uptake. Taking into account the 5 μM EGTA present in the medium, the [Ca^{2+}] obtained after calcium addition was 15 μM. The rate of mitochondrial calcium uptake was calculated from the rate of decrease in the extramitochondrial [Ca^{2+}] after calcium addition.

3. Results

3.1. Kinetics and Na^+ dependence of Ca^{2+}-release from mitochondria

We have first studied the kinetics of Ca^{2+} release from mitochondria. We have loaded mitochondria with Ca^{2+} by making a short perfusion with a Ca^{2+}-containing intracellular medium. After that, Ca^{2+}-free medium was perfused to initiate Ca^{2+} release. Panel A of Fig. 1 shows that perfusion of the EGTA-containing medium triggered a very fast Ca^{2+}-release, at a rate similar to that seen during the Ca^{2+} entry period in the presence of 7 μM [Ca^{2+}]. The right trace in this panel shows the Ca^{2+} release obtained when the EGTA-containing medium was devoid of Na^+. It can be appreciated that blocking Ca^{2+}-release through the mitochondrial Na^+/Ca^{2+} exchanger produced a very significant decrease in the rate of Ca^{2+} release. Panel B shows mean data of several similar experiments, showing the effect of the absence of Na^+ on the kinetics of Ca^{2+} release from mitochondria. Panel C shows the dependence of the rate of Ca^{2+} release on the mitochondrial [Ca^{2+}] both in the presence and in the absence of Na^+. Data in panel B were polynomial fitted to smooth them. Then, Ca^{2+} exit rate data were obtained as the first derivative of the fitted traces, and finally the obtained rates were plotted against the $[Ca^{2+}]_M$ corresponding to each measured rate. The figure shows that the rate

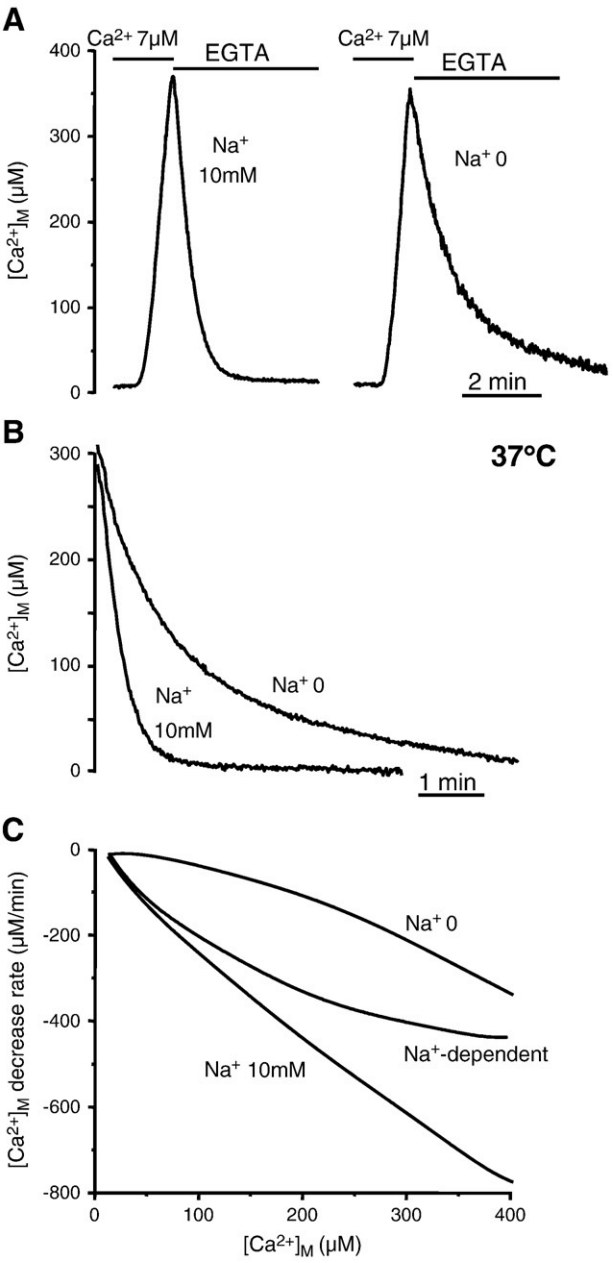

Fig. 1. Kinetics of mitochondrial Ca^{2+} release at 37 °C. HeLa cells expressing mitmutAEQ and reconstituted with coelenterazine n were permeabilized and stimulated briefly with a 7 μM [Ca^{2+}] buffer, as indicated in the panel A. Then, an EGTA-containing intracellular medium was perfused to monitor Ca^{2+} release from mitochondria, both in the presence and in the absence of 10 mM [Na^+]. Panel B shows a superimposition of the release curves in the presence and in the absence of 10 mM [Na^+] obtained as the mean of 6 different experiments of each kind. Panel C shows the dependence of the rate of Ca^{2+} release on the mitochondrial [Ca^{2+}]. The mean data of panel B were polynomial fitted and the first derivative of these curves was plotted against the $[Ca^{2+}]_M$. The curve labelled Na^+-dependent was obtained by subtracting the Na^+ 0 curve from the Na^+ 10 mM curve.

of Ca^{2+} release increased linearly with the $[Ca^{2+}]_M$ in the presence of Na^+, reaching rates around 800 μM/min at 400 μM $[Ca^{2+}]_M$. Instead, in the absence of Na^+, the rate was very small at $[Ca^{2+}]_M$ below 200 μM, and then started to increase in a non-linear mode. As a result of that, the rate of Na^+-dependent Ca^{2+} release, obtained as the subtraction of both curves, saturated at $[Ca^{2+}]_M$ around 400 μM.

In conclusion, the Na^+-dependent Ca^{2+} release pathway is clearly predominant at $[Ca^{2+}]_M$ below 200 μM and is nearly the only Ca^{2+}-exit pathway at $[Ca^{2+}]_M$ below 100 μM. In contrast, the Na^+-independent Ca^{2+}-exit pathway rapidly activates at $[Ca^{2+}]_M$ above 200 μM and approaches the rate of the Na^+-dependent pathway when the $[Ca^{2+}]_M$ reaches 400 μM. Because of aequorin consumption, we could not measure the rates at higher $[Ca^{2+}]_M$, but the data point to a further increase in the importance of the Na^+-independent pathway at higher $[Ca^{2+}]_M$ because of the saturation of the Na^+-dependent pathway.

Regarding the Ca^{2+}-release rates obtained, values in the literature are usually reported in terms of nmol Ca^{2+}·mg protein^{-1}·min^{-1}. Taking into account that the relationship between mitochondrial matrix protein concentration and water volume is about 1 mg protein·μl water^{-1} or 1000 mg·ml^{-1} [16,17], a good approximation to transform our data (μM·min^{-1} or nmol·ml^{-1}·min^{-1}) into those units would be just dividing by this protein concentration, so that 1000 μM/min corresponds to a free Ca^{2+} exit rate of 1 nmol free Ca^{2+}·mg protein^{-1}·min^{-1}. Of course, our data only measure the fluxes of free Ca^{2+}, so that the total calcium flux should be much higher depending on the mitochondrial Ca^{2+} buffering. However, transforming our data into those units (nmol free Ca^{2+}·mg protein^{-1}·min^{-1}) is useful because it allows obtaining information about mitochondrial Ca^{2+} buffering by comparing the free Ca^{2+} flux rates obtained here, with the values in the literature for the total calcium fluxes (see the Discussion). Thus, according to our data, the Na^+-dependent Ca^{2+} efflux pathway saturates below 500 μM/min or 0.5 nmol free Ca^{2+}·mg protein^{-1}·min^{-1}, while the Na^+-independent Ca^{2+} efflux pathway is much slower at low $[Ca^{2+}]_M$ but approaches also those values at $[Ca^{2+}]_M$ above 400 μM.

3.2. Effect of the temperature on Ca^{2+} release

We have then investigated the effect of the temperature on the rates of Ca^{2+} release from mitochondria. Fig. 2 shows the kinetics of Ca^{2+} release from mitochondria at 22 °C and in the presence of several different Na^+ concentrations. Because of the slower consumption of aequorin at low temperature, it is now possible to monitor the release rates at higher $[Ca^{2+}]_M$. Panel A of Fig. 2 shows that Ca^{2+} release was

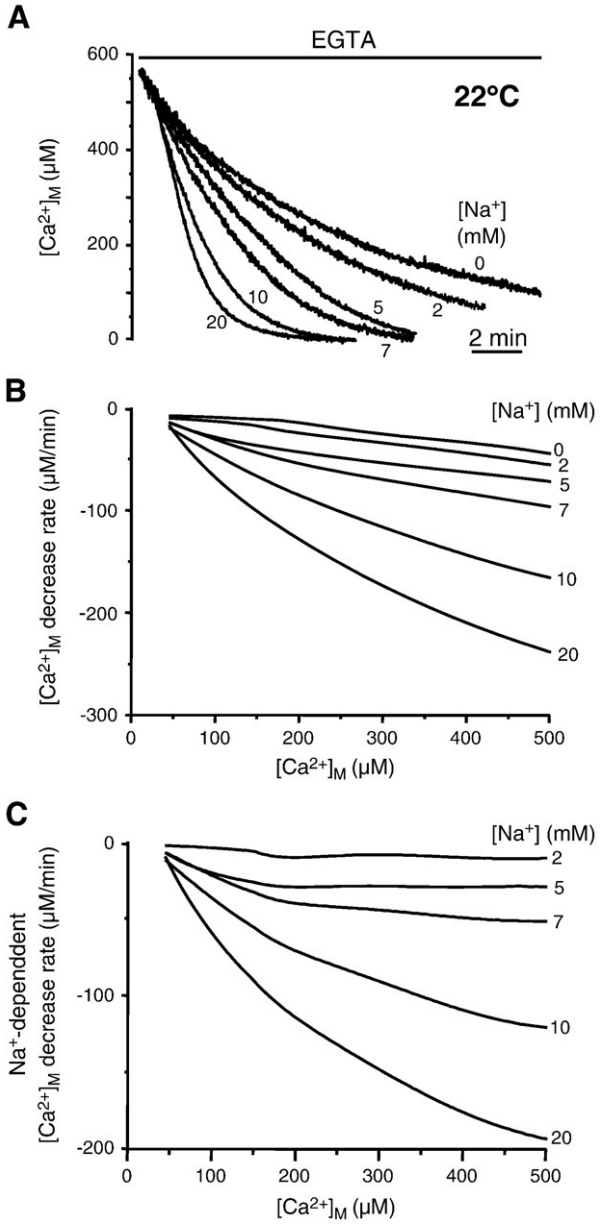

Fig. 2. Kinetics of mitochondrial Ca^{2+} release at 22 °C. HeLa cells expressing mitmutAEQ and reconstituted with coelenterazine n were permeabilized, stimulated briefly with a 7 μM $[Ca^{2+}]$ buffer and then perfused with an EGTA-containing intracellular medium in the presence of different $[Na^+]$, as indicated in the figure. Panel A shows the mean Ca^{2+} release curves obtained in 4–8 similar experiments of each kind. Panel B shows the dependence of the rate of Ca^{2+} release on the mitochondrial $[Ca^{2+}]$ obtained as in Fig. 1. Panel C shows the Na^+-dependent Ca^{2+} release obtained by subtracting the Na^+ 0 curve in panel B from each of the other curves.

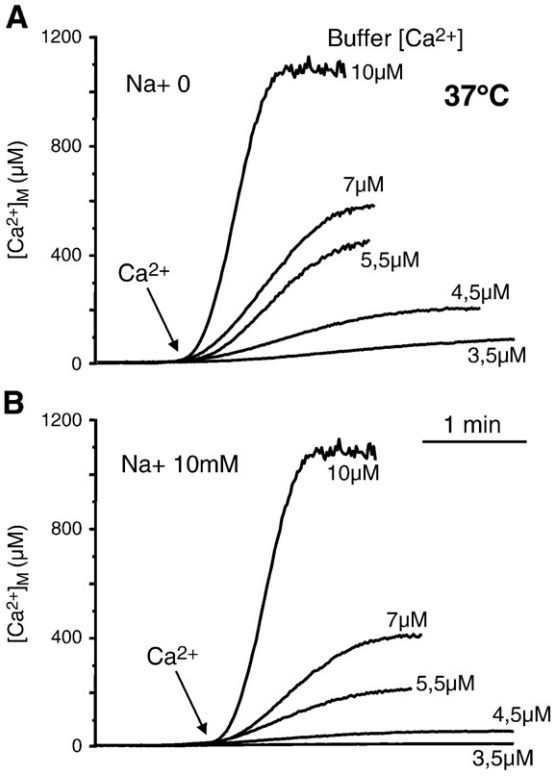

Fig. 3. Kinetics of mitochondrial Ca^{2+} uptake at 37 °C and different cytosolic $[Ca^{2+}]$ and $[Na^+]$. HeLa cells expressing mitmutAEQ and reconstituted with coelenterazine n were permeabilized and then stimulated with $[Ca^{2+}]$ buffers containing different $[Ca^{2+}]$, as indicated in the figure. Panel A, intracellular perfusion solutions without sodium. Panel B, solutions containing 10 mM $[Na^+]$. Data are the mean of 3–5 different experiments of each kind.

much slower here than at 37 °C (compare with Fig. 1) and it was also dramatically dependent on the $[Na^+]$ in the intracellular medium. In panel B of this figure, data have been transformed to show the dependence of the Ca^{2+} exit rate on $[Ca^{2+}]_M$, and in panel C the curve obtained in the absence of Na^+ has been subtracted from the rest to show only the Na^+-dependent Ca^{2+}-exit rate.

Several conclusions can be obtained from these data. First, the Na^+-independent Ca^{2+}-exit pathway was very small at all the $[Ca^{2+}]_M$ values and it hardly reached values of 40 μM/min (0.04 nmol free Ca^{2+}·mg protein^{-1}·min^{-1}) at 500 μM $[Ca^{2+}]_M$. Therefore, the exit rates observed through the Na^+-independent Ca^{2+}-exit pathway decreased by more than 10-fold when the temperature was reduced from 37 °C to 22 °C. Second, the rate of Ca^{2+} release through the Na^+-dependent Ca^{2+}-exit pathway was also sensitive to the temperature, although the dependence was smaller. For a $[Na^+]$ of 10 mM, the maximum rate observed at 22 °C was about 4-fold smaller than at 37 °C, that is, about 120 μM/min or 0.12 nmol free Ca^{2+}·mg protein^{-1}·min^{-1}. As a consequence, Ca^{2+}-release from mitochondria at 22 °C in standard Na^+-containing medium is more than 4-fold slower than at 37 °C and is mainly mediated by the Na^+-dependent pathway at every $[Ca^{2+}]_M$. Finally, regarding the Na^+-dependence of Ca^{2+} release, the data of panel C of Fig. 2 show that the $[Na^+]$ producing half-maximal activation is about 10 mM. Sigmoidal fitting of the rate values obtained at 400 μM $[Ca^{2+}]_M$ for each $[Na^+]$ gave an EC_{50} value of 9.5 ± 0.6 mM.

3.3. Kinetics of Ca^{2+} uptake by mitochondria

We have now analyzed the kinetics of Ca^{2+} increase in mitochondria in the presence of different $[Ca^{2+}]$ and at every temperature. Fig. 3 shows Ca^{2+}-entry traces obtained after perfusion of intracellular medium containing different $[Ca^{2+}]$ to permeabilized cells, both in the absence (panel A) and in the presence (panel B) of 10 mM $[Na^+]$. The rate of Ca^{2+} entry increased with the $[Ca^{2+}]$ in the medium, and the increase was dramatically accelerated when medium $[Ca^{2+}]$ was above 7 μM. In fact, perfusion of 10 μM $[Ca^{2+}]$ triggered a very fast increase in $[Ca^{2+}]_M$ that rapidly reached the millimolar range. The presence of 10 mM $[Na^+]$ considerably reduced the rate of uptake, but the effect was much stronger at low buffer $[Ca^{2+}]$, 7 μM or below. In contrast, the rate of Ca^{2+} entry was little dependent on the presence of Na^+ when the medium $[Ca^{2+}]$ reached 10 μM.

Fig. 4 shows the dependence of the Ca^{2+} increase rate, obtained in experiments as those of Fig. 3, with $[Ca^{2+}]_M$. Several experiments as those of Fig. 3 were pooled and polynomial fitted, and the first derivative in each case was plotted against $[Ca^{2+}]_M$. Rate values corresponding to the increasing slope part of the uptake curves (before the maximum rate in each case is reached) were not included for clarity. Panels A and B show data obtained in the absence of Na^+ (panel B is an expansion of panel A in both scales). Panels C and D show data obtained in the presence of 10 mM $[Na^+]$ (panel D is an

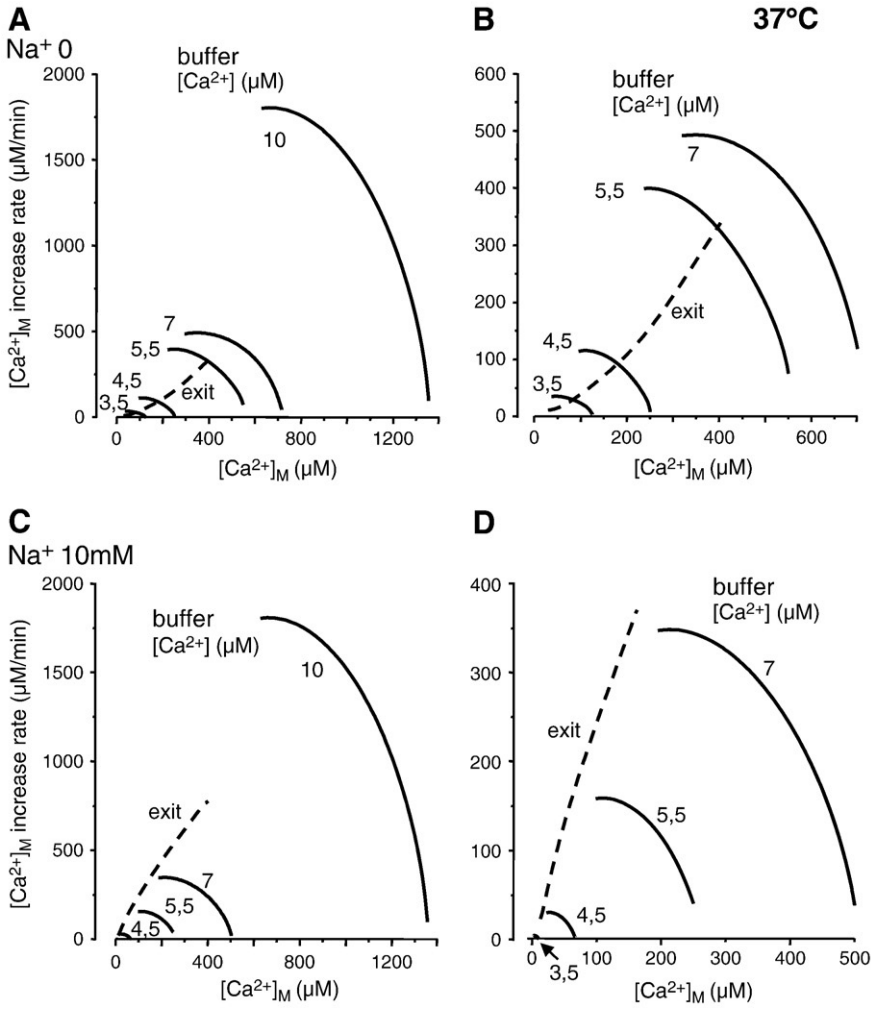

Fig. 4. Dependence of the mitochondrial $[Ca^{2+}]$ increase rate at 37 °C on $[Ca^{2+}]_M$. Data in Fig. 3 were transformed as described in Fig. 1 to plot the rate of mitochondrial $[Ca^{2+}]$ increase (balance between influx and efflux rates) against $[Ca^{2+}]_M$ at every cytosolic $[Ca^{2+}]$ and both in the absence of $[Na^+]$ (panels A and B, which is an expansion of panel A) and in the presence of 10 mM $[Na^+]$ (panels C and D, which is an expansion of panel C). The dashed curves represent the rate of Ca^{2+} release in each case, taken from Fig. 1.

expansion of panel C). The dashed lines show for comparison the rates of Ca^{2+}-exit in each case, taken from Fig. 1.

The curves of Fig. 4 do not show unidirectional Ca^{2+}-entry into mitochondria, but the balance between mitochondrial Ca^{2+} influx and Ca^{2+} efflux for each medium $[Ca^{2+}]$ and intramitochondrial $[Ca^{2+}]$. The presence of Na^+ in the medium shifts down the curves obtained at low $[Ca^{2+}]$ (up to 7 μM), because of the increased Ca^{2+} exit flux through the Na^+/Ca^{2+} exchanger. However, Ca^{2+} entry through the uniporter should remain the same, and that was the case. To calculate unidirectional Ca^{2+} entry, we can study the steady-state in the Ca^{2+} entry curves, that is, the region where $[Ca^{2+}]_M$ is stable because Ca^{2+} influx and Ca^{2+} efflux are equal. In the curves of Fig. 4, that region corresponds to the intersection with the *X* axis, when the rate is 0, and the Ca^{2+} entry rate corresponding to each particular curve should then be equal to the exit rate at the $[Ca^{2+}]_M$ in the intersection. Fig. 5 exemplifies the calculation and shows that Ca^{2+} entry is independent of the presence of Na^+. Extrapolation of the curves for 4.5 and 5.5 μM $[Ca^{2+}]$ in the presence and in the absence of Na^+ provides the $[Ca^{2+}]_M$ where Ca^{2+} influx and efflux are balanced in each case. At that point, the Ca^{2+} efflux rate should be equal to the Ca^{2+} influx, and can be obtained from the efflux curve. The figure shows that Ca^{2+} influx at 4.5 μM medium $[Ca^{2+}]$ was about 160 μM/min, and at 5.5 μM medium $[Ca^{2+}]$ was about 650 μM/min, and those values were independent of the presence of Na^+ in the medium, in spite of the large difference in the rate curves in both cases.

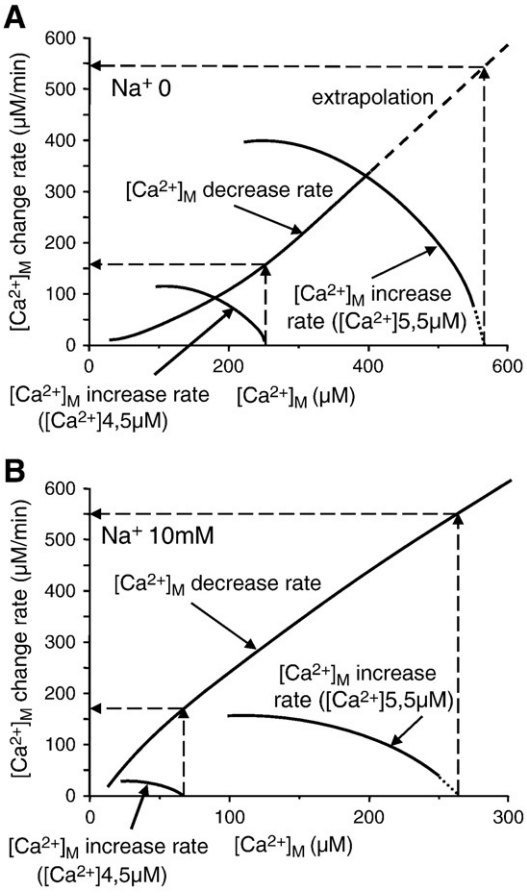

Fig. 5. Calculation of unidirectional Ca^{2+} influx rates. The figure shows data from Fig. 4 corresponding to the curves of $[Ca^{2+}]_M$ increase rate (balance between influx and efflux rates) at 4.5 μM $[Ca^{2+}]$ and 5.5 μM $[Ca^{2+}]$ both in the absence (panel A) and in the presence (panel B) of 10 mM $[Na^+]$, together with the $[Ca^{2+}]_M$ decrease rates in both cases. When the $[Ca^{2+}]_M$ increase rate curves reach the *X* axis, influx and efflux must be equal and the pure influx rate can be calculated from the value of the $[Ca^{2+}]_M$ decrease rate curve obtained at the same intramitochondrial $[Ca^{2+}]$ (as indicated by the dashed arrows).

The maximum rate of mitochondrial Ca^{2+} increase observed with the 10 μM buffer $[Ca^{2+}]$ was about 1800 μM/min, corresponding to about 1.8 nmol free $Ca^{2+} \cdot mg\ protein^{-1} \cdot min^{-1}$, and it was independent of the presence of Na^+. The reason for that may be that, as shown in Fig. 1, the Na^+-dependent Ca^{2+} exit pathway saturated at $[Ca^{2+}]_M$ around 400 μM, and above that concentration the Na^+-independent Ca^{2+} exit pathway started to be predominant. Thus, at the high $[Ca^{2+}]_M$ reached in the presence of the 10 μM Ca^{2+} buffer, the contribution of the Na^+-dependent Ca^{2+} exit pathway should be small. It is difficult to estimate the maximum Ca^{2+} entry rate with the 10 μM $[Ca^{2+}]$ buffer as we did in Fig. 5, because we would need to make a very large extrapolation of the Ca^{2+}-exit rate. However, we can obtain a more direct estimation by adding the maximum measured rate value (1800 μM/min), obtained at a $[Ca^{2+}]_M$ of 700 μM, with the extrapolation of the Ca^{2+} exit rates up to that point (800–1000 μM/min), obtaining a total value of about 2600–2800 μM/min or 2.6–2.8 nmol free $Ca^{2+} \cdot mg\ protein^{-1} \cdot min^{-1}$.

Regarding the lower $[Ca^{2+}]$ buffers, particularly below 5 μM, probably the cytosolic $[Ca^{2+}]$ found under most physiological conditions of cell stimulation, the Ca^{2+}-entry rates were much smaller and in the same range as Ca^{2+}-exit rates. Thus, the observed Ca^{2+} increase under those conditions was largely dependent on the presence of Na^+ in the medium and could be significantly modulated by changes in $[Na^+]$. Fig. 6 shows the effect of the presence of different $[Na^+]$ in the perfusion medium on the $[Ca^{2+}]_M$ increase induced by a 4.5 μM $[Ca^{2+}]$ buffer. Panel A shows the crude uptake curves and panel B shows the dependence of the rate of Ca^{2+}-increase on $[Ca^{2+}]_M$. Both the maximum rate of $[Ca^{2+}]_M$ increase and the steady-state

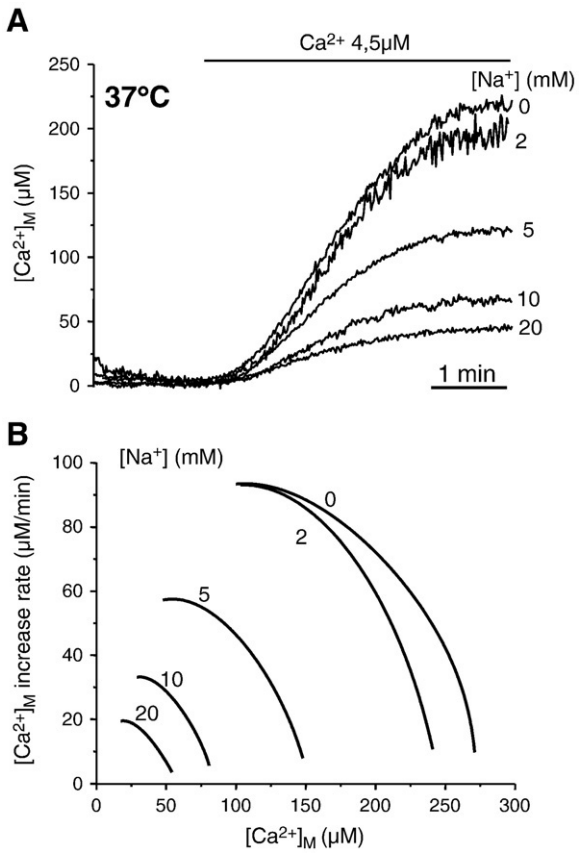

Fig. 6. Effect of $[Na^+]$ on mitochondrial $[Ca^{2+}]$ increase rate at 37 °C. HeLa cells expressing mitmutAEQ and reconstituted with coelenterazine n were permeabilized and then stimulated with a 4.5 μM $[Ca^{2+}]$ buffer in the presence of different $[Na^+]$, as indicated in the figure. Panel A shows a typical experiment. In panel B, mean data from 4 to 7 experiments of each kind were transformed as described in Fig. 1 to plot the rate of mitochondrial Ca^{2+} increase against $[Ca^{2+}]_M$ at every $[Na^+]$.

$[Ca^{2+}]_M$ obtained in the absence of Na^+ was decreased by 5-fold in the presence of 20 mM $[Na^+]$, and the larger changes occurred in the physiological range of intracellular $[Na^+]$, around 5 mM. Sigmoidal fit of the effects of $[Na^+]$ on either the steady-state $[Ca^{2+}]_M$ values or the maximum rates of Ca^{2+} efflux provided values for the mean effect of $[Na^+]$ of 4.6 ± 0.1 mM and 5.3 ± 0.4 mM, respectively.

3.4. Effect of the temperature on Ca^{2+} uptake

We have then investigated the balance between Ca^{2+} entry and Ca^{2+} release at 22 °C. Fig. 7 shows the kinetics of the increase in $[Ca^{2+}]_M$ induced by the addition of different buffered $[Ca^{2+}]$ to permeabilized cells, both in the presence and in the absence of Na^+, and Fig. 8 shows the relationship between the Ca^{2+} increase rate and the $[Ca^{2+}]_M$ in each case. The dashed traces represent the Ca^{2+} exit rates at both 0 and 10 mM Na^+, taken from Fig. 2. As occurred at 37 °C, the presence of Na^+ reduced the rates obtained at $[Ca^{2+}]$ below 7 μM, hardly affecting the rate obtained with a 10 μM $[Ca^{2+}]$ buffer. The maximum rate obtained with a 10 μM $[Ca^{2+}]$ buffer could be calculated by adding the maximum rate measured (at 200–400 μM $[Ca^{2+}]_M$) with the exit rate at that $[Ca^{2+}]_M$, obtaining a value of 1100–1200 μM/min or 1.1–1.2 nmol free Ca^{2+}·mg protein^{-1}·min^{-1}, about 2.5-fold smaller than the rate measured at 37 °C for the same $[Ca^{2+}]$. However, because the effect of the temperature on the release rates is larger (more than 4-fold, see Figs. 1 and 2), the final steady-state $[Ca^{2+}]_M$ reached at 22 °C was higher than at 37 °C for the $[Ca^{2+}]$ buffers below 7 μM (compare Figs. 3 and 7).

3.5. Total mitochondrial Ca^{2+} uptake

We have finally studied the rate of total mitochondrial Ca^{2+} uptake obtained in mitochondria isolated from HeLa cells and stimulated with a calcium bolus under conditions similar to those of the previous experiments, but using the dye Calcium Green 5 N to measure the decrease in extramitochondrial $[Ca^{2+}]$ induced by mitochondrial Ca^{2+} uptake. We are aware that this method is unable to measure the maximal rate of mitochondrial Ca^{2+} uptake, because of the limitations imposed by the changes in membrane potential occurring during mitochondrial Ca^{2+} uptake, that lead to serious underestimations of the rate of uptake [2,6]. However, the results are useful as a lower estimation for the rate of total calcium uptake by HeLa cell mitochondria.

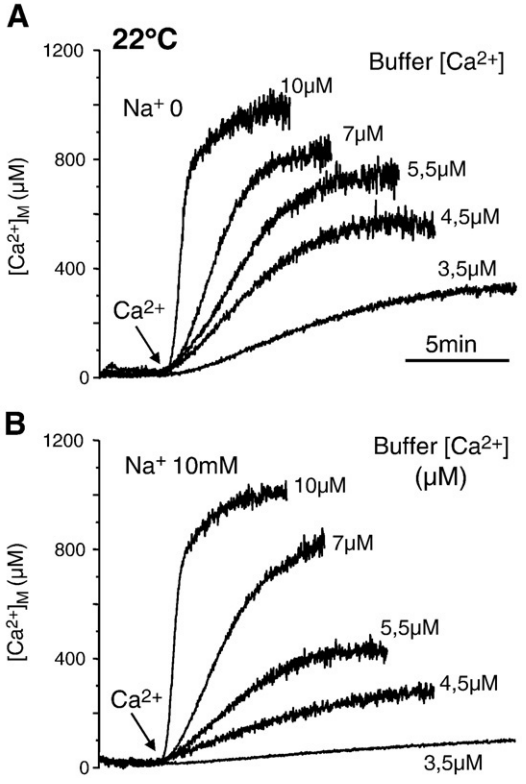

Fig. 7. Kinetics of mitochondrial Ca^{2+} uptake at 22 °C and different cytosolic $[Ca^{2+}]$ and $[Na^+]$. HeLa cells expressing mitmutAEQ and reconstituted with coelenterazine n were permeabilized and then stimulated with $[Ca^{2+}]$ buffers containing different $[Ca^{2+}]$, as indicated in the figure, and either in the absence (panel A) or in the presence (panel B) of 10 mM $[Na^+]$. Data are the mean of 2 different experiments of each kind.

Fig. 9 shows that addition of a Ca^{2+} bolus of 150 nmol total calcium·mg protein^{-1} (15 μM $[Ca^{2+}]$) produced a sudden increase in the $[Ca^{2+}]$ measured by the extramitochondrial dye, which then progressively decreased in the next few minutes until all the added calcium had been taken up by mitochondria. In several similar experiments, the rate of total calcium uptake measured at an extramitochondrial $[Ca^{2+}]$ of 10 μM was 21 ± 3 nmol total calcium·mg protein^{-1}·min^{-1} (mean ± s.e., n = 5).

4. Discussion

We have made a detailed study of the kinetics of mitochondrial Ca^{2+} fluxes by measuring the mitochondrial $[Ca^{2+}]$ in permeabilized cells during Ca^{2+} entry and Ca^{2+} release in the presence of different extramitochondrial $[Ca^{2+}]$ and $[Na^+]$, and different temperatures. Our study provides a view of the dynamics of intramitochondrial $[Ca^{2+}]$ along the activation of mitochondrial Ca^{2+} fluxes and allows making a direct comparative estimation of the balance between Ca^{2+} entry and Ca^{2+} release fluxes. In addition it provides new information on mitochondrial Ca^{2+} buffering.

4.1. Mitochondrial Ca^{2+} uptake rates and matrix Ca^{2+} buffering

The maximum activity of the Ca^{2+} uniporter has been estimated in rat liver mitochondria to be around 1400 and 900 nmol total Ca^{2+}·mg protein^{-1}·min^{-1} at 30 °C and 20 °C, respectively, using conditions of constant membrane potential [2,6,7]. The presence of 1 mM Mg^{2+} should reduce these figures by about 20–30%, to values close to 1000 and 600 nmol total Ca^{2+}·mg protein^{-1}·min^{-1}, respectively. In our experiments, the measured rate of total calcium uptake was 21 nmol total calcium·mg protein^{-1}·min^{-1} in the presence of about 10 μM extramitochondrial $[Ca^{2+}]$. Reported values for the Km for Ca^{2+} of the uniporter are in the 20–50 μM range [1–9], and previous data indicate that the maximum rate should be at least 4-fold higher than that obtained at 10 μM $[Ca^{2+}]$ [4,5]. Therefore, a reasonable estimation for the maximum rate of uptake in our conditions would be about 80 nmol total calcium·mg protein^{-1}·min^{-1}. This rate is about 10-fold smaller than that previously obtained in rat liver mitochondria, although we should remember that it is a lower estimation for the actual rate, because of the changes in membrane potential occurring during mitochondrial Ca^{2+} uptake [2,6]. In conclusion, the rate of total calcium uptake at 37 °C in our cells should be in the range 100–1000 nmol total calcium·mg protein^{-1}·min^{-1}.

Regarding the rates of free Ca^{2+} uptake obtained from the aequorin experiments, we obtain uptake rates with a 10 μM $[Ca^{2+}]$ buffer of 2.8 and 1.2 nmol free Ca^{2+}·mg protein^{-1}·min^{-1} at 37 °C and 22 °C, respectively. Using the same factor as above (4-fold), a reasonable estimation for the maximum uptake rate of free Ca^{2+} in our case would be 10 nmol free Ca^{2+}·mg protein^{-1}·min^{-1} at 37 °C and 5 nmol free Ca^{2+}·mg protein^{-1}·min^{-1} at 22 °C. These values for the rate of free Ca^{2+} increase in mitochondria are 10- to 100-fold smaller than the above-mentioned rates for total calcium uptake by mitochondria. The difference should be due to the mitochondrial buffering capacity and would therefore represent a good estimation for the Ca^{2+} bound/Ca^{2+} free relationship in the mitochondrial matrix along the Ca^{2+} uptake process. If this is correct, the Ca^{2+}

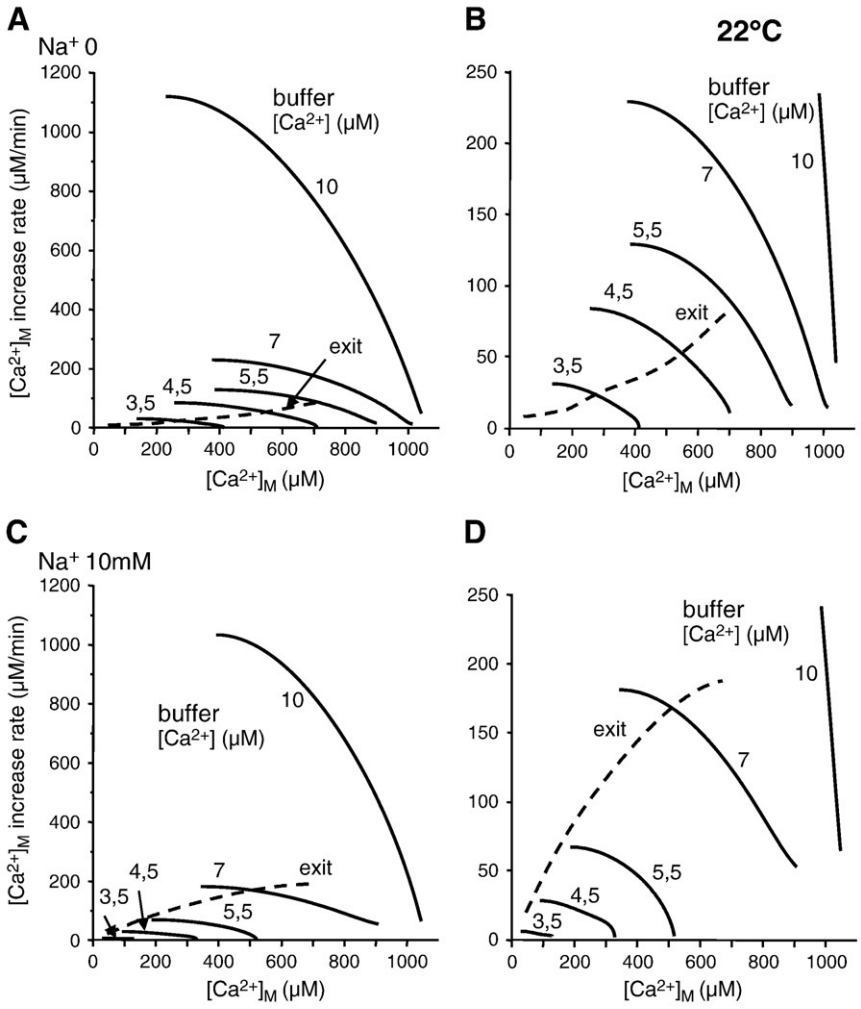

Fig. 8. Dependence of the mitochondrial [Ca^{2+}] increase rate at 22 °C on $[Ca^{2+}]_M$. Data in Fig. 3 were transformed as described in Fig. 1 to plot the rate of mitochondrial Ca^{2+} increase (balance between influx and efflux rates) against $[Ca^{2+}]_M$ at every cytosolic [Ca^{2+}] and both in the absence of [Na^+] (panels A and B, which is an expansion of panel A) and in the presence of 10 mM [Na^+] (panels C and D, which is an expansion of panel C). The dashed curves represent the rate of Ca^{2+} release in each case, taken from Fig. 2.

bound/Ca^{2+} free ratio in the mitochondria would be similar to that measured in the cytosol of many cells [3,18], although this parameter may depend on the cell type [19]. Previous estimations for the Ca^{2+} binding ratio in the mitochondrial matrix range from 4000 [20] to 150,000 [21]. The discrepancy with these figures is mainly due to the different values obtained for the free [Ca^{2+}] inside mitochondria during Ca^{2+} loading, a problem which has been discussed before [13].

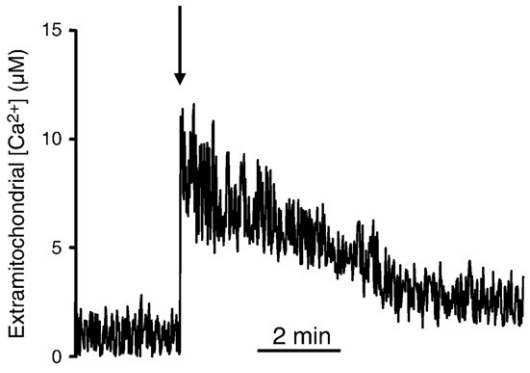

Fig. 9. Total calcium uptake by mitochondria isolated from HeLa cells. 0.1 mg of protein from the HeLa cell mitochondrial preparation were suspended in 1 ml of intracellular medium containing 5 μM EGTA and 0.3 μM Calcium Green-5 N at 37 °C. When indicated by the arrow, 20 nmol of calcium (final [Ca^{2+}] 15 μM) was added to start mitochondrial Ca^{2+} uptake. This experiment is representative of 5 similar ones.

Regarding mitochondrial Ca^{2+} buffering, our data show smooth free Ca^{2+} increase curves up to the millimolar range in mitochondria exposed to a constant rate of Ca^{2+} uptake. Similarly, Ca^{2+} release curves show a nice exponential kinetics from about 500 μM to resting values. Therefore, our data do not show any evidence for high affinity Ca^{2+} buffering in the low micromolar range in mitochondria. Rather, our data are consistent with previous data [22,23] suggesting the presence of a high-capacity and low affinity Ca^{2+} buffering. This buffering would allow rapid uptake and release of large amounts of Ca^{2+} from mitochondria, with $[Ca^{2+}]_M$ transiently reaching the tens or even hundreds of micromolar range, as we have previously shown in intact chromaffin cells [4]. If the factor of two orders of magnitude for the bound/free calcium relationship is correct, then reaching a $[Ca^{2+}]_M$ of 1 mM would correspond to a net calcium load of 100 nmol total $Ca^{2+}\cdot$mg protein^{-1}. Interestingly, this value corresponds approximately to the maximum amount of calcium that can be accumulated by mitochondria within the classically considered limited loading, which is reversible and does not produce damage to mitochondria [8,24]. In the presence of phosphate, mitochondria is known to be able to store 10–30 times more calcium than that [21,24], accompanied by irreversible damage, morphological changes and calcium phosphate precipitation. Our data suggest that, contrarily to previous estimations [21,25], this precipitation only occurs when the free $[Ca^{2+}]_M$ approaches the

millimolar range and thus the limited loading threshold. Then, the free $[Ca^{2+}]_M$ stabilizes around 1 mM (as in Figs. 3 and 7) while calcium phosphate precipitation develops.

4.2. Mitochondrial Ca^{2+} release rates

Regarding Ca^{2+} release from mitochondria, the maximum rate of the Na^+/Ca^{2+} exchange system was 0.5 nmol free $Ca^{2+}\cdot$mg protein$^{-1}\cdot$min^{-1} at 37 °C and 0.12 nmol free $Ca^{2+}\cdot$mg protein$^{-1}\cdot$min^{-1} at 22 °C. Values in the literature for the maximum rate of this system range between 2.6 and 18 nmol total $Ca^{2+}\cdot$mg protein$^{-1}\cdot$min^{-1} at room temperature [6,7,26,27]. Again here, our values for the rate of free Ca^{2+} release are smaller by a factor of about 20–150 than the published values for total Ca^{2+} release through this system. In the case of the Na^+-independent Ca^{2+} release flux, our values for the maximum rate of this system are about 0.5 and 0.04 nmol free $Ca^{2+}\cdot$mg protein$^{-1}\cdot$min^{-1} at 37 °C and 22 °C, respectively. The published values for the maximum rate of this system have been obtained at room temperature and are around 1–2 nmol total $Ca^{2+}\cdot$mg protein$^{-1}\cdot$min^{-1} [6,7,23]. In this case the total flux is 25- to 50-fold larger than the free Ca^{2+} flux measured here. At this respect, it is interesting to note that in our experiments the Na^+-independent Ca^{2+} efflux was very slow at low $[Ca^{2+}]_M$, below 200 μM, and its rate increased at higher $[Ca^{2+}]_M$. However, it has been reported that this efflux system saturates at total mitochondrial calcium values around 25 nmol total $Ca^{2+}\cdot$mg protein^{-1} [23], which according to the data in this paper (relationship bound Ca^{2+}/free Ca^{2+} of 100 in the matrix and assuming 1 μl water/mg protein) should correspond to a $[Ca^{2+}]_M$ of around 250 μM. A possible explanation for the discrepancy would be the activation of a new pathway for Ca^{2+} release from mitochondria when $[Ca^{2+}]_M$ rises above these values, perhaps a reversible or transient opening of the mitochondrial permeability transition.

Ca^{2+}-release from mitochondria in HeLa cells was highly dependent on the extramitochondrial $[Na^+]$, particularly at $[Ca^{2+}]_M$ below 100–200 μM. In fact, at 100 μM $[Ca^{2+}]_M$, 85–90% of Ca^{2+} release was dependent of the presence of Na^+. The $[Na^+]$ required for half-maximal activation of Ca^{2+} release was about 10 mM (Fig. 2), although the $[Na^+]$ required for half-maximal inhibition of the $[Ca^{2+}]_M$ increase rate (Fig. 6) was smaller, close to 5 mM. The difference may be due to the experimental design or perhaps also to the temperature. In any case, these values are comparable with reported values for the Km of this system, which are in the range of 2.6 to 9.4 mM [27–29]. This $[Na^+]$ is in the physiological range, so that physiological variations in the cytosolic $[Na^+]$ may produce significant variations in Ca^{2+} accumulation by mitochondria, as it has been previously proposed [29]. Our data show that the rate of Ca^{2+} release from mitochondria is comparable with the rate of Ca^{2+} entry when the cytosolic $[Ca^{2+}]$ keeps below 7 μM, which is the case for most physiological cell stimulations, with the possible exception of local high-Ca^{2+} microdomains. Therefore, modulation by cytosolic $[Na^+]$ of the rate of Ca^{2+} release from mitochondria may be physiologically relevant for mitochondrial Ca^{2+} homeostasis.

4.3. Temperature dependence of mitochondrial Ca^{2+} fluxes

Finally, our data show also a very important dependence of mitochondrial Ca^{2+} release with the temperature. Na^+-dependent Ca^{2+}-release increased its activity by 4-fold when the temperature was increased from 22 °C to 37 °C, and Na^+-independent Ca^{2+}-release increased its activity by more than 10-fold in the same interval. This temperature dependence is larger than that of the Ca^{2+}-entry mechanism, which increases its rate only about twice by the same temperature increase. Because of that, the final $[Ca^{2+}]_M$ reached at steady-state was higher at 22 °C than at 37 °C in the presence of every $[Ca^{2+}]$ buffer, except for the 10 μM $[Ca^{2+}]$ one, which leads to saturation of the probe at around 1 mM $[Ca^{2+}]_M$ and also probably to calcium phosphate precipitation. It is very important to have into account this large temperature dependence of the mitochondrial Ca^{2+}-release mechanisms to interpret previous data in the literature regarding mitochondrial Ca^{2+} storage ability during physiological cell function. In fact, most of the original work on the role of mitochondria in Ca^{2+} homeostasis was made at room temperature [20,30–33]. Those papers grounded the key idea that mitochondria constitute a very important transient Ca^{2+} buffer able to modulate cytosolic $[Ca^{2+}]$ homeostasis. However, regarding the kinetics of that phenomenon, one of their conclusions was that mitochondria was able to take up Ca^{2+} rapidly during cell activation and then release it slowly, thus generating a mitochondrial Ca^{2+} transient much prolonged than the cytosolic one and a sustained Ca^{2+} release from mitochondria well after the original $[Ca^{2+}]_c$ transient had finished. That is in fact the case at room temperature, but the kinetics of this phenomenon under physiological conditions is very different. The rate of mitochondrial Ca^{2+}-release at 37 °C is much faster, and the kinetics of the mitochondrial $[Ca^{2+}]$ transient is in fact very similar to that of the cytosolic one, but with very different amplitude [4]. This point is physiologically very important, as the response of mitochondrial $[Ca^{2+}]$ to rapid $[Ca^{2+}]_c$ oscillations, such as those occurring in cardiac cells, either generating $[Ca^{2+}]_M$ oscillations or progressive $[Ca^{2+}]_M$ accumulation [34–36], may critically depend on that.

4.4. Conclusion

In conclusion, our data reveal mitochondria as a highly dynamic compartment in terms of Ca^{2+} homeostasis, able to take up and release Ca^{2+} fast enough to follow the cytosolic Ca^{2+} transients, but undergoing reversible variations in $[Ca^{2+}]_M$ that could span up to four orders of magnitude, from 100 nM to 1 mM. Under physiological conditions, of course, the $[Ca^{2+}]_M$ transients in most of the mitochondria are surely smaller, but the organelle has the capacity to do it and mitochondria close to high Ca^{2+} microdomains may be involved in such a big Ca^{2+} movements.

Acknowledgments

This work was supported by grants from Ministerio de Educación y Ciencia (BFU2008-01871) and from Junta de Castilla y León (VA103A08 and GR105). Sergio de la Fuente holds an FPI (Formación de Personal Investigador) fellowship from the Spanish Ministerio de Ciencia e Innovación and Pablo Montenegro holds a JAE (Junta de Ampliación de Estudios) predoctoral fellowship from Consejo Superior de Investigaciones Cientificas (CSIC). We thank Pilar Alvarez and Laura González for excellent technical assistance.

References

[1] A. Vinogradov, A. Scarpa, The initial velocities of calcium uptake by rat liver mitochondria, J. Biol. Chem. 248 (1973) 5527–5531.
[2] M. Bragadin, T. Pozzan, G.F. Azzone, Kinetics of Ca^{2+} carrier in rat liver mitochondria, Biochemistry 18 (1979) 5972–5978.
[3] T. Xu, M. Naraghi, H. Kang, E. Neher, Kinetic studies of Ca^{2+} binding and Ca^{2+} clearance in the cytosol of adrenal chromaffin cells, Biophys. J. 73 (1997) 532–545.
[4] M. Montero, M.T. Alonso, E. Carnicero, I. Cuchillo-Ibañez, A. Albillos, A.G. Garcia, J. Garcia-Sancho, J. Alvarez, Chromaffin-cell stimulation triggers fast millimolar mitochondrial Ca^{2+} transients that modulate secretion, Nat. Cell Biol. 2 (2000) 57–61.
[5] Y. Kirichok, G. Krapivinsky, D.E. Clapham, The mitochondrial calcium uniporter is a highly selective ion channel, Nature 427 (2004) 360–364.
[6] P. Bernardi, Mitochondrial transport of cations: channels, exchangers, and permeability transition, Physiol. Rev. 79 (1999) 1127–1155.
[7] R. Rizzuto, P. Bernardi, T. Pozzan, Mitochondria as all-round players of the calcium game, J. Physiol. 529 (2000) 37–47.
[8] T.E. Gunter, D.R. Pfeiffer, Mechanisms by which mitochondria transport calcium, Am. J. Physiol. 258 (1990) C755–C786.
[9] T.E. Gunter, S.S. Sheu, Characteristics and possible functions of mitochondrial Ca^{2+} transport mechanisms, Biochim. Biophys. Acta. 1787 (2009) 1291–1308.
[10] M.J. Barrero, M. Montero, J. Alvarez, Dynamics of $[Ca^{2+}]$ in the endoplasmic reticulum and cytoplasm of intact HeLa cells. A comparative study, J. Biol. Chem. 272 (1997) 27694–27699.

[11] M. Montero, C.D. Lobatón, A. Moreno, J. Alvarez, A novel regulatory mechanism of the mitochondrial Ca^{2+} uniporter revealed by the p38 mitogen-activated protein kinase inhibitor SB202190, FASEB J. 16 (2002) 1955–1957.
[12] M. Montero, M.J. Barrero, J. Alvarez, [Ca^{2+}] microdomains control agonist-induced Ca^{2+} release in intact HeLa cells, FASEB J. 11 (1997) 881–885.
[13] L. Vay, E. Hernández-SanMiguel, C.D. Lobatón, A. Moreno, M. Montero, J. Alvarez, Mitochondrial free [Ca^{2+}] levels and the permeability transition, Cell Calcium 45 (2009) 243–250.
[14] J. Llopis, J.M. McCaffery, A. Miyawaki, M.G. Farquhar, R.Y. Tsien, Measurement of cytosolic, mitochondrial, and Golgi pH in single living cells with green fluorescent proteins, Proc. Natl. Acad. Sci. U. S. A. 95 (1998) 6803–6808.
[15] M.F. Cano-Abad, G. Di Benedetto, P.J. Magalhães, L. Filippin, T. Pozzan, Mitochondrial pH monitored by a new engineered green fluorescent protein mutant, J. Biol. Chem. 279 (2004) 11521–11529.
[16] C.R. Hackenbrock, Chemical and physical fixation of isolated mitochondria in low-energy and high-energy states, Proc. Natl. Acad. Sci. U. S. A. 61 (1968) 598–605.
[17] A.D. Beavis, R.D. Brannan, K.D. Garlid, Swelling and contraction of the mitochondrial matrix. I. A structural interpretation of the relationship between light scattering and matrix volume, J. Biol. Chem. 260 (1985) 13424–13433.
[18] J.R. Berlin, J.W.M. Bassani, D.M. Bers, Intrinsic cytosolic calcium buffering properties of single rat cardiac myocytes, Biophys. J. 67 (1994) 1775–1787.
[19] H. Mogami, J. Gardner, O.V. Gerasimenko, P. Camello, O.H. Petersen, A.V. Tepikin, Calcium binding capacity of the cytosol and endoplasmic reticulum of mouse pancreatic acinar cells, J. Physiol. (Lond.) 518.2 (1999) 463–467.
[20] D.F. Babcock, J. Herrington, Y.-B. Park, B. Hille, Mitochondrial participation in the intracellular Ca^{2+} network, J. Cell Biol. 136 (1997) 833–843.
[21] S. Chalmers, D.G. Nicholls, The relationship between free and total calcium concentrations in the matrix of liver and brain mitochondria, J. Biol. Chem. 278 (2003) 19062–19070.
[22] K.E. Coll, S.K. Joseph, B.E. Corkey, J.R. Williamson, Determination of the matrix free Ca^{2+} concentration and kinetics of Ca^{2+} efflux in liver and heart mitochondria, J. Biol. Chem. 257 (1982) 8696–8704.
[23] D.E. Wingrove, T.E. Gunter, Kinetics of mitochondrial calcium transport. I. Characteristics of the sodium-independent calcium efflux mechanism of liver mitochondria, J. Biol. Chem. 261 (1986) 15159–15165.
[24] A.L. Lehninger, Mitochondria and calcium ion transport, Biochem. J. 119 (1970) 129–138.
[25] D.G. Nicholls, Mitochondria and calcium signalling, Cell Calcium 38 (2005) 311–317.
[26] M. Crompton, R. Moser, H. Lüdi, E. Carafoli, The interrelations between the transport of sodium and calcium in mitochondria of various mammalian tissues, Eur. J. Biochem. 82 (1978) 25–31.
[27] D.E. Wingrove, T.E. Gunter, Kinetics of mitochondrial calcium transport. II. A kinetic description of the sodium-dependent calcium efflux mechanism of liver mitochondria and inhibition by ruthenium red and by tetraphenylphosphonium, J. Biol. Chem. 261 (1986) 15166–15171.
[28] D.A. Cox, M.A. Matlib, A role for the mitochondrial Na^{+}-Ca^{2+} exchanger in the regulation of oxidative phosphorylation in isolated heart mitochondria, J. Biol. Chem. 268 (1993) 938–947.
[29] M. Sedova, L.A. Blatter, Intracellular sodium modulates mitochondrial calcium signaling in vascular endothelial cells, J. Biol. Chem. 275 (2000) 35402–35407.
[30] S.A. Thayer, R.J. Miller, Regulation of the intracellular free calcium concentration in single rat dorsal root ganglion neurones in vitro, J. Physiol. (Lond.) 425 (1990) 85–115.
[31] R.J. White, I.J. Reynolds, Mitochondria accumulate Ca^{2+} following intense glutamate stimulation of cultured rat forebrain neurons, J. Physiol. (Lond.) 498 (1997) 31–47.
[32] Y.B. Park, J. Herrington, D.F. Babcock, B. Hille, Ca^{2+} clearance mechanisms in isolated rat adrenal chromaffin cells, J. Physiol. (Lond.) 492 (1996) 329–346.
[33] J. Herrington, Y.B. Park, D.F. Babcock, B. Hille, Dominant role of mitochondria in clearance of large Ca^{2+} loads from rat adrenal chromaffin cells, Neuron 16 (1996) 219–228.
[34] Z. Zhou, M.A. Matlib, D.M. Bers, Cytosolic and mitochondrial Ca^{2+} signals in patch clamped mammalian ventricular myocytes, J. Physiol. (Lond.) 507 (1998) 379–403.
[35] V. Robert, P. Gurlini, V. Tosello, T. Nagai, A. Miyawaki, F. Di Lisa, T. Pozzan, Beat-to-beat oscillations of mitochondrial [Ca^{2+}] in cardiac cells, EMBO J. 20 (2001) 4998–5007.
[36] E.N. Dedkova, L.A. Blatter, Mitochondrial Ca^{2+} and the heart, Cell Calcium 44 (2008) 77–91.